

Synthesis, crystal structure and Hirshfeld surface analysis of *N*-(6-acetyl-1-nitronaphthalen-2-yl)-acetamide

Xin-Wei Shi,^a Shao-Jun Zheng,^b Qiang-Qiang Lu,^a Gen Li^a and Ya-fu Zhou^{a*}

^aXi'an Botanical Garden of Shaanxi Province (Institute of Botany of Shaanxi Province), Shaanxi Engineering Research Centre for Conservation and Utilization of Botanical Resources, Xi'an 710061, People's Republic of China, and ^bSchool of Environmental and Chemical Engineering, Jiangsu University of Science and Technology, Zhenjiang 212003, Jiangsu, People's Republic of China. *Correspondence e-mail: yafu-zhou@xab.ac.cn

Received 20 November 2023

Accepted 18 February 2024

Edited by A. Briceno, Venezuelan Institute of Scientific Research, Venezuela

Keywords: crystal structure; naphthalene ring; hydrogen bonding; Hirshfeld surface analysis.

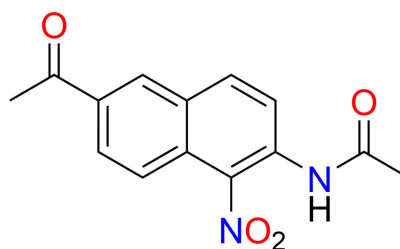
CCDC reference: 2333518

Supporting information: this article has supporting information at journals.iucr.org/e

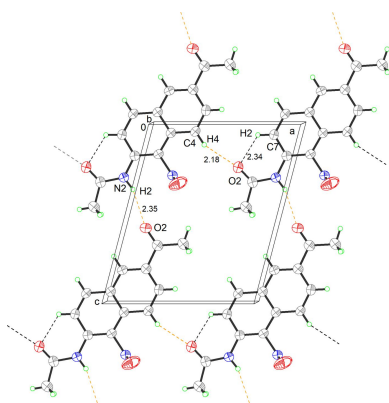
The title compound, C₁₄H₁₂N₂O₄, was obtained from 2-acetyl-6-aminonaphthalene through two-step reactions of acetylation and nitration. The molecule comprises the naphthalene ring system consisting of functional systems bearing a acetyl group (C-2), a nitro group (C-5), and an acetilamino group (C-6). In the crystal, the molecules are assembled into two-dimensional sheet-like structures by intermolecular N—H···O and C—H···O hydrogen-bonding interactions. Hirshfeld surface analysis illustrates that the most important contributions to the crystal packing are from O···H/H···O (43.7%), H···H (31.0%), and C···H/H···C (8.5%) contacts.

1. Chemical context

Organic small molecules with naphthalene ring systems are attractive photonic materials due to their high photoluminescence quantum efficiency, color tunability, and size-dependent optical properties (Wang *et al.*, 2012; Yao *et al.*, 2013). Modifying the organic molecular structure can tune the intermolecular hydrogen-bonding and π – π stacking interactions, which influence their packing mode during self-assembly and determine the final aggregated structures. The molecular stacking patterns in crystals can affect asymmetric light propagation (Yagai *et al.*, 2012; Zou *et al.*, 2018; Zhang *et al.*, 2018).



The title compound (**I**), *N*-(6-acetyl-1-nitronaphthalen-2-yl)acetamide, obtained from 2-acetyl-6-aminonaphthalene through two-step reactions of acetylation and nitration, is a Prodan fluorescent dye with red fluorescence and a large Stoke shift (Xu *et al.*, 2017). The stacking of naphthalene compounds into crystals depends on intermolecular hydrogen bonds and π – π stacking interactions. The nitro group and the acetilamino group of the naphthalene ring system will affect intermolecular interactions, making it possible to change the one- or two-dimensional stacking arrangement, which in turn



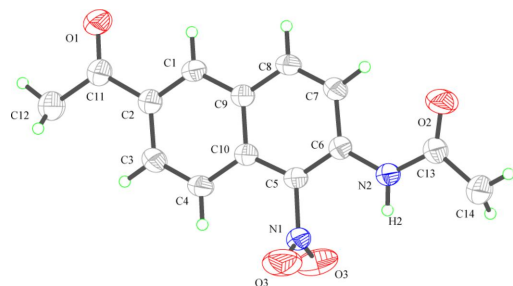


Figure 1

The molecular structure of the title compound (I) with the atomic numbering scheme. Displacement ellipsoids are depicted at the 50% probability level.

affects photo-ion conduction (Eya'ane Meva *et al.*, 2012; Nguyen *et al.*, 2004).

2. Structural commentary

The molecular structure of the title compound (I) is shown in Fig. 1. The molecules are semi-rigid and almost fully coplanar, except for the nitro oxygen atoms and methyl hydrogen atoms. Notably, compound (I) has a primary amine group on the naphthalene core, while the reactant has a secondary amine at the same position. It may have more steric repulsion with neighboring molecules compared to the reactant when assembled into 2D structures. Self-assembly of naphthalene framework organic molecules through π - π stacking forms 3D sheet-like structures with uniform dimensions.

In compound (I), the nitro group and acetylamino group are adjacent, located at positions C-5 and C-6, respectively, and

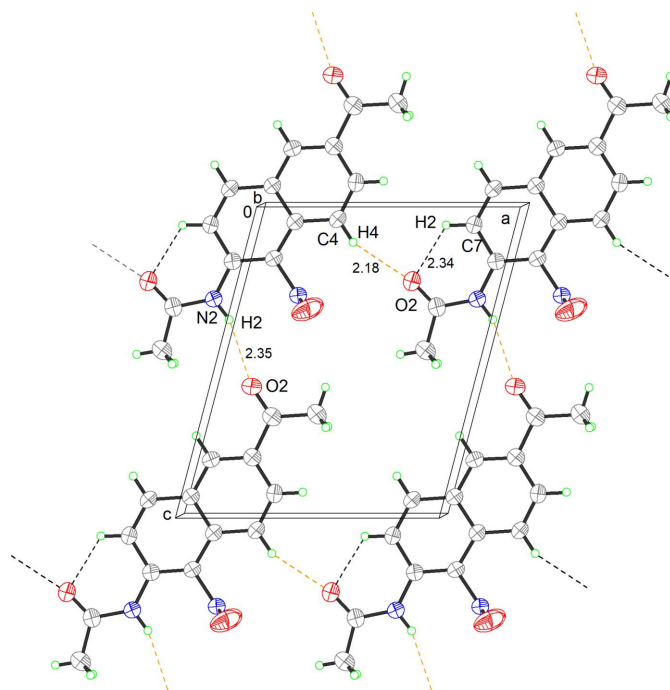


Figure 2

The packing of molecules in the title compound (I), viewed along the *b*-axis direction (N2—H2...O1 hydrogen bonds are shown as orange dashed lines, C7—H7...O2 and C4—H4...O2 hydrogen bonds are shown as gray dashed lines).

Table 1

Hydrogen-bond geometry (\AA , $^\circ$).

<i>D</i> —H... <i>A</i>	<i>D</i> —H	H... <i>A</i>	<i>D</i> ... <i>A</i>	<i>D</i> —H... <i>A</i>
N2—H2...O1 ⁱ	0.86	2.35	3.177 (2)	161
C7—H7...O2	0.93	2.18	2.792 (2)	123
C4—H4...O2 ⁱⁱ	0.93	2.34	3.219 (2)	157

Symmetry codes: (i) *x*, *y*, *z* + 1; (ii) *x* + 1, *y*, *z*.

the acetyl group is located at the 2-position of the naphthalene ring system. The angle between the two oxygen atoms on the nitro group located at positions C-5 is $123.93 (18)^\circ$, and the torsion angles C6—C5—N1—O3 and C10—C5—N1—O3 are $-90.34 (15)$ and $89.66 (15)^\circ$, respectively. The angles of the acetyl group at the 2-position, O1—C11—C2 and O1—C11—C12, are $120.13 (18)$ and $120.52 (18)^\circ$, respectively. In addition, the dihedral angle between the nitro group and the plane through the naphthalene ring system is $89.66 (15)^\circ$.

3. Supramolecular features

In the crystal, a unit cell contains four molecules, which exhibit a centrosymmetric arrangement (Fig. 2), and hydrogen bonding and π - π stacking interactions were responsible for the formation of the crystal structures with distinct morphologies.

The growth pattern for the title compound (I) is a 1D wire-like structure and hydrogen bonding advances the growth along the *a*-axis direction. The molecules are linked *via* N2—H2...O1 hydrogen bonds, generating 2D layers propagating along the [010] axis direction (Table 1). Without hydrogen-bonding and other strong interactions between molecules in adjacent layers, π - π stacking interactions, with centroid-centroid distances of 3.67 \AA , are the predominant driving force during self-assembly, which facilitates the crystal of the title compound growth along the [010] direction, forming a 3D structure (Meva *et al.*, 2012; Nguyen *et al.*, 2004). Weak C4—H4...O2 contacts are also observed.

4. Hirshfeld Surface analysis

A Hirshfeld surface analysis was performed and the associated fingerprint plots, which provide a 2D view of the intermolecular interactions within molecular crystals, were gener-

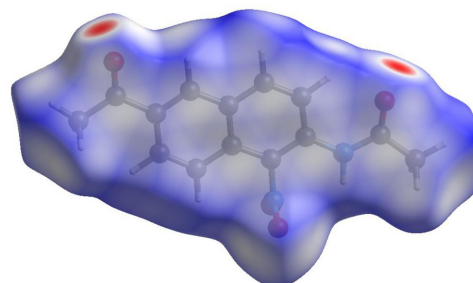


Figure 3

Front view of the three-dimensional Hirshfeld surface of the title compound (I) mapped over d_{norm} .

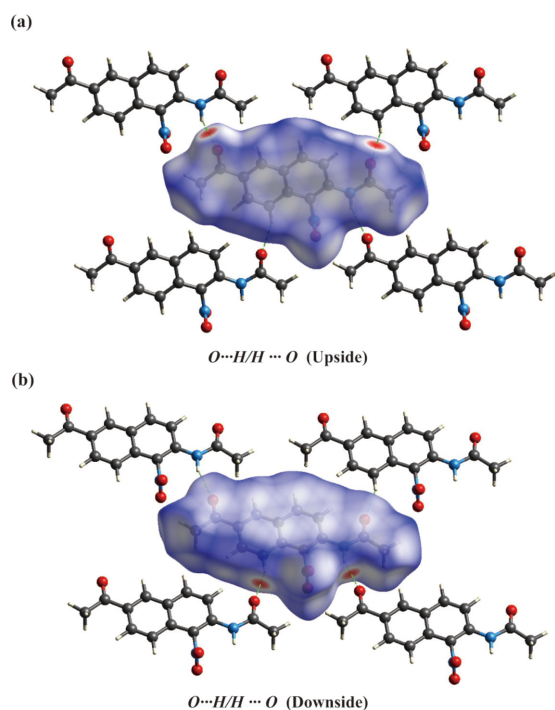


Figure 4
Hirshfeld surface mapped over d_{norm} for the title compound (I) showing: $H \cdots O/O \cdots H$ (upside and downside) contacts.

ated using *Crystal Explorer 21.5* (Spackman *et al.*, 2021), with a standard resolution of the 3D d_{norm} surfaces plotted over a fixed color scale of -0.1253 (red) to 1.4046 (blue) arbitrary units (Fig. 3). The $N2-H2 \cdots O1$ hydrogen bond was identified to be a crucial structure-forming interaction within the crystal packing. The intense red spots symbolizing short contacts and negative d_{norm} values on the surface are related to the presence of the $N2-H2 \cdots O1$ hydrogen bonds in the crystal structure. The weak $C4-H4 \cdots O2$ contacts are indicated by faint red spots (Fig. 4).

The 2D fingerprint plots for the $H \cdots O/O \cdots H$, $H \cdots H$, $H \cdots C/C \cdots H$, and $H \cdots N/N \cdots H$ contacts are shown in Fig. 5. The most significant interactions are $H \cdots O/O \cdots H$, which play a defining role in the overall crystal packing, contributing 43.7%, and are located in the tip and middle region of the fingerprint plot. $H \cdots H$ interactions contribute 31.0%, being located in the middle region of the fingerprint plot. The contributions of the weak $H \cdots C/C \cdots H$ and $H \cdots N/N \cdots H$ contacts to the Hirshfeld surface are 8.5 and 1.1%, respectively.

Shape-index and curvedness are the metrics that describe the local shape in terms of principal curvatures, representing the surface properties of the crystal molecule to determine their arrangements. The Hirshfeld surface mapped over electrostatic potential, shape-index, curvedness and fragment patches is shown in Fig. 6. The electrostatic potential map (Fig. 6a) highlights the electronegative (red) and electro-positive (blue) regions in the molecule. The molecule shows red colored regions near the oxygen atom (O1), indicating the electronegative spots (Akhileshwari *et al.*, 2021). The pattern of red and blue triangles on the shape-index map (Fig. 6b)

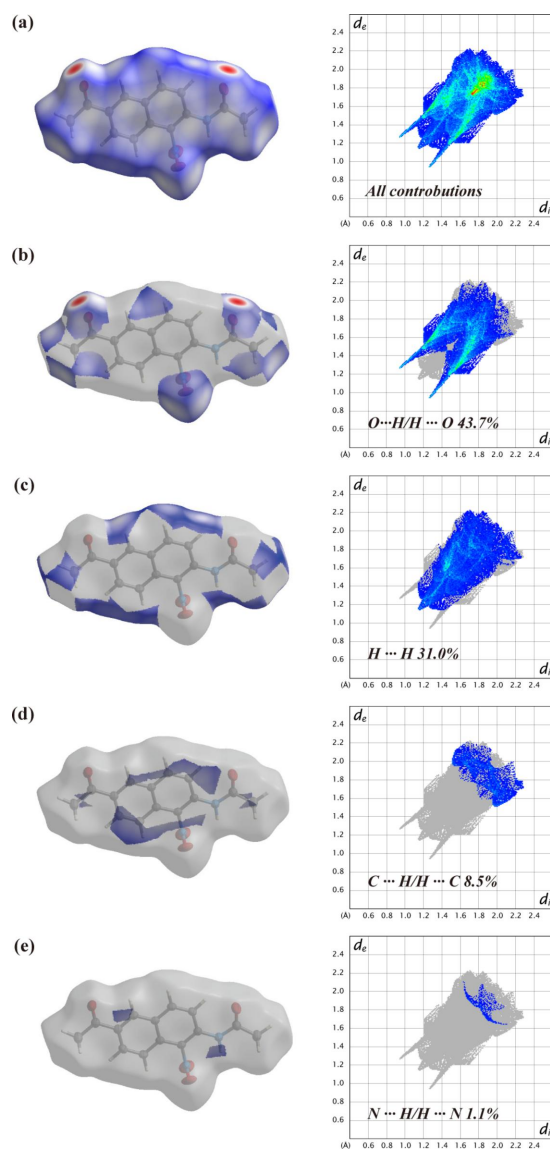
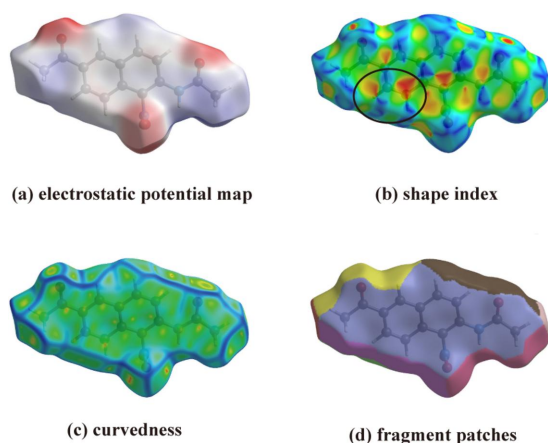


Figure 5
The two-dimensional fingerprint plots of the title compound (I), showing (a) all interactions, and delineated into (b) $H \cdots H$, (c) $O \cdots H/H \cdots O$, (d) $C \cdots H/H \cdots C$, and (e) $N \cdots H/H \cdots N$ interactions [The d_e and d_i values represent the distances (in Å) from a point on the Hirshfeld surface to the nearest atoms inside and outside the surface, respectively.]

shows feature characteristic of π - π interactions. As the molecule shows flat regions on the curvedness map (Fig. 6c), it is evident that the title molecule is arranged in planar stacking (Spackman & Jayatilaka, 2009). The fragment patches (Fig. 6d) illustrates the coordination number of the corresponding atoms in the compound.

5. Synthesis and crystallization

1.0 g of 2-acetyl-6-aminonaphthalene were dissolved in 35 ml of Ac_2O , stirred for 10 minutes, and 30 ml of CH_3COOH were added, followed by the slow addition of 6.5 ml of concentrated HNO_3 under ice-bath conditions for 3 h at room temperature. When the reaction was complete, it is extracted with CH_2Cl_2

**Figure 6**

Hirshfeld surface of the title compound (I) mapped over (a) electrostatic potential, (b) shape-index, (c) curvedness, and (d) fragment patches.

three times, the organic phase was combined, the positive silica gel column was passed under normal pressure after spinning (eluent CH_2Cl_2 :ethyl acetate, 10:1). The eluent containing the product components was collected and the light-yellow solid was concentrated. It was dissolved in methanol and placed in a refrigerator at 277 to cultivate light-yellow transparent square crystals (Xu *et al.*, 2017). The MeOH was dissolved and red transparent square crystals suitable for X-ray diffraction were obtained at 277 K in the refrigerator.

6. Refinement

Crystal data, data collection and structure refinement details are summarized in Table 2. H atoms were positioned geometrically ($\text{C-H} = 0.93\text{--}0.95 \text{ \AA}$) and allowed to ride on their parent atoms, with $U_{\text{iso}}(\text{H}) = 1.2 U_{\text{eq}}(\text{C})$ or $1.5 U_{\text{eq}}(\text{C-methyl})$.

Acknowledgements

The authors thank Hubei Normal University and Nian Zhao for recording the X-ray crystallographic data for the crystals.

Funding information

Funding for this research was provided by: the Xi'an Science and Technology Plan Project (grant No. 20NYF0043); the Key Research and Development Program of Shaanxi (grant No. 2023-YBNY-248 and 2023-YBNY-100); the Key Research and Development Program of China (grant No. 2021YFD1600400); the National Natural Science Foundation of China (grant No. 42301053).

References

Akhileshwari, P., Kiran, K. R., Sridhar, M. A., Sadashiva, M. P. & Lokanath, N. K. (2021). *J. Mol. Struct.* **1242**, 130747.

Table 2

Experimental details.

Crystal data	
Chemical formula	$\text{C}_{14}\text{H}_{12}\text{N}_2\text{O}_4$
M_r	272.26
Crystal system, space group	Monoclinic, $P2_1/m$
Temperature (K)	293
a, b, c (Å)	8.7649 (14), 6.8899 (11), 10.6868 (18)
β (°)	104.676 (4)
V (Å ³)	624.31 (18)
Z	2
Radiation type	Mo $K\alpha$
μ (mm ⁻¹)	0.11
Crystal size (mm)	0.22 × 0.20 × 0.18
Data collection	
Diffractometer	Bruker CCD
Absorption correction	Multi-scan (SADABS; Krause <i>et al.</i> , 2015)
No. of measured, independent and observed [$I > 2\sigma(I)$] reflections	4087, 1229, 1079
R_{int}	0.016
$(\sin \theta/\lambda)_{\text{max}}$ (Å ⁻¹)	0.599
Refinement	
$R[F^2 > 2\sigma(F^2)]$, $wR(F^2)$, S	0.043, 0.124, 1.07
No. of reflections	1229
No. of parameters	118
H-atom treatment	H-atom parameters constrained
$\Delta\rho_{\text{max}}$, $\Delta\rho_{\text{min}}$ (e Å ⁻³)	0.21, -0.29

Computer programs: SMART and SAINT (Bruker, 2002), SHELXT2014/7 (Sheldrick, 2015a), SHELXL2014/7 (Sheldrick, 2015b), SHELXTL (Sheldrick, 2008) and publCIF (Westrip, 2010).

Bruker (2002). SAINT and SMART. Bruker AXS Inc., Madison, Wisconsin, USA.

Eya'ane Meva, F., Schaarschmidt, D., Abdulmalic, M. A. & Rüffer, T. (2012). *Acta Cryst.* **E68**, o3460–o3461.

Krause, L., Herbst-Irmer, R., Sheldrick, G. M. & Stalke, D. (2015). *J. Appl. Cryst.* **48**, 3–10.

Nguyen, T. Q., Martel, R., Avouris, P., Bushey, M. L., Brus, L. & Nuckolls, C. (2004). *J. Am. Chem. Soc.* **126**, 5234–5242.

Sheldrick, G. M. (2008). *Acta Cryst.* **A64**, 112–122.

Sheldrick, G. M. (2015a). *Acta Cryst.* **A71**, 3–8.

Sheldrick, G. M. (2015b). *Acta Cryst.* **C71**, 3–8.

Spackman, M. A. & Jayatilaka, D. (2009). *CrystEngComm*, **11**, 19–32.

Spackman, P. R., Turner, M. J., McKinnon, J. J., Wolff, S. K., Grimwood, D. J., Jayatilaka, D. & Spackman, M. A. (2021). *J. Appl. Cryst.* **54**, 1006–1011.

Wang, Y., Liu, J., Tran, H. D., Mecklenburg, M., Guan, X. N., Stieg, A. Z., Regan, B. C., Martin, D. C. & Kaner, R. B. (2012). *J. Am. Chem. Soc.* **134**, 9251–9262.

Westrip, S. P. (2010). *J. Appl. Cryst.* **43**, 920–925.

Xu, Z., Zheng, S. & Liu, Y. (2017). China patent, CN106866437 A.

Yagai, S., Goto, Y., Lin, X., Karatsu, T., Kitamura, A., Kuzuhara, D., Yamada, H., Kikkawa, Y., Saeki, A. & Seki, S. (2012). *Angew. Chem.* **124**, 6747–6751.

Yao, W., Yan, Y. L., Xue, L., Zhang, C., Li, G. P., Zheng, Q. D., Zhao, Y. S., Jiang, H. & Yao, J. N. (2013). *Angew. Chem. Int. Ed.* **52**, 8713–8717.

Zhang, C., Dong, H. & Zhao, Y. (2018). *Adv. Opt. Mater.* **6**, 1701193.

Zou, T., Wang, X., Ju, H., Zhao, L., Guo, T., Wu, W. & Wang, H. (2018). *Crystals*, **8**, 22.

supporting information

Acta Cryst. (2024). E80 [https://doi.org/10.1107/S2056989024001609]

Synthesis, crystal structure and Hirshfeld surface analysis of *N*-(6-acetyl-1-nitronaphthalen-2-yl)acetamide

Xin-Wei Shi, Shao-Jun Zheng, Qiang-Qiang Lu, Gen Li and Ya-fu Zhou

Computing details

N-(6-Acetyl-1-nitronaphthalen-2-yl)acetamide

Crystal data

$C_{14}H_{12}N_2O_4$

$M_r = 272.26$

Monoclinic, $P2_1/m$

$a = 8.7649$ (14) Å

$b = 6.8899$ (11) Å

$c = 10.6868$ (18) Å

$\beta = 104.676$ (4)°

$V = 624.31$ (18) Å³

$Z = 2$

$F(000) = 284$

$D_x = 1.448$ Mg m⁻³

Mo $K\alpha$ radiation, $\lambda = 0.71073$ Å

Cell parameters from 1846 reflections

$\theta = 2.4\text{--}25.0^\circ$

$\mu = 0.11$ mm⁻¹

$T = 293$ K

Block, red

$0.22 \times 0.20 \times 0.18$ mm

Data collection

Bruker CCD

diffractometer

phi and ω scans

Absorption correction: multi-scan
(SADABS; Krause *et al.*, 2015)

4087 measured reflections

1229 independent reflections

1079 reflections with $I > 2\sigma(I)$

$R_{\text{int}} = 0.016$

$\theta_{\text{max}} = 25.2^\circ$, $\theta_{\text{min}} = 2.0^\circ$

$h = -9 \rightarrow 10$

$k = -8 \rightarrow 7$

$l = -12 \rightarrow 12$

Refinement

Refinement on F^2

Least-squares matrix: full

$R[F^2 > 2\sigma(F^2)] = 0.043$

$wR(F^2) = 0.124$

$S = 1.07$

1229 reflections

118 parameters

0 restraints

Hydrogen site location: mixed

H-atom parameters constrained

$w = 1/[\sigma^2(F_o^2) + (0.0709P)^2 + 0.1248P]$

where $P = (F_o^2 + 2F_c^2)/3$

$(\Delta/\sigma)_{\text{max}} < 0.001$

$\Delta\rho_{\text{max}} = 0.21$ e Å⁻³

$\Delta\rho_{\text{min}} = -0.29$ e Å⁻³

Special details

Geometry. All esds (except the esd in the dihedral angle between two l.s. planes) are estimated using the full covariance matrix. The cell esds are taken into account individually in the estimation of esds in distances, angles and torsion angles; correlations between esds in cell parameters are only used when they are defined by crystal symmetry. An approximate (isotropic) treatment of cell esds is used for estimating esds involving l.s. planes.

Fractional atomic coordinates and isotropic or equivalent isotropic displacement parameters (\AA^2)

	<i>x</i>	<i>y</i>	<i>z</i>	$U_{\text{iso}}^*/U_{\text{eq}}$
C1	0.0705 (2)	0.7500	−0.18378 (17)	0.0351 (4)
H1	−0.0097	0.7500	−0.2598	0.042*
C2	0.2243 (2)	0.7500	−0.19094 (18)	0.0376 (5)
C3	0.3449 (2)	0.7500	−0.07463 (19)	0.0438 (5)
H3	0.4497	0.7500	−0.0786	0.053*
C4	0.3117 (2)	0.7500	0.04290 (19)	0.0416 (5)
H4	0.3934	0.7500	0.1179	0.050*
C5	0.1084 (2)	0.7500	0.16916 (16)	0.0319 (4)
C6	−0.0450 (2)	0.7500	0.17851 (17)	0.0323 (4)
C7	−0.1648 (2)	0.7500	0.06065 (18)	0.0384 (5)
H7	−0.2703	0.7500	0.0626	0.046*
C8	−0.1267 (2)	0.7500	−0.05469 (18)	0.0378 (5)
H8	−0.2076	0.7500	−0.1303	0.045*
C9	0.0307 (2)	0.7500	−0.06439 (17)	0.0321 (4)
C10	0.1533 (2)	0.7500	0.05139 (17)	0.0320 (4)
C11	0.2589 (2)	0.7500	−0.32103 (19)	0.0423 (5)
C12	0.4260 (3)	0.7500	−0.3295 (2)	0.0620 (7)
H12A	0.4321	0.7500	−0.4154	0.074*
H12B	0.4769	0.6362	−0.2882	0.074*
C13	−0.2245 (2)	0.7500	0.3252 (2)	0.0440 (5)
C14	−0.2240 (3)	0.7500	0.4642 (2)	0.0561 (6)
H14A	−0.3152	0.7500	0.4775	0.067*
H14B	−0.1689	0.8561	0.5077	0.067*
N1	0.23711 (18)	0.7500	0.28778 (14)	0.0398 (4)
N2	−0.07930 (18)	0.7500	0.29967 (15)	0.0389 (4)
H2	0.0005	0.7500	0.3659	0.047*
O1	0.15177 (18)	0.7500	−0.41834 (14)	0.0603 (5)
O2	−0.34453 (19)	0.7500	0.24224 (16)	0.0925 (8)
O3	0.28721 (15)	0.5958 (2)	0.33316 (11)	0.0761 (5)

Atomic displacement parameters (\AA^2)

	U^{11}	U^{22}	U^{33}	U^{12}	U^{13}	U^{23}
C1	0.0347 (10)	0.0390 (10)	0.0289 (9)	0.000	0.0032 (7)	0.000
C2	0.0365 (10)	0.0409 (10)	0.0359 (10)	0.000	0.0099 (8)	0.000
C3	0.0297 (9)	0.0613 (13)	0.0407 (11)	0.000	0.0091 (8)	0.000
C4	0.0291 (9)	0.0583 (13)	0.0340 (10)	0.000	0.0020 (7)	0.000
C5	0.0314 (9)	0.0328 (9)	0.0292 (9)	0.000	0.0032 (7)	0.000
C6	0.0333 (9)	0.0313 (9)	0.0321 (9)	0.000	0.0079 (7)	0.000
C7	0.0284 (9)	0.0498 (11)	0.0363 (10)	0.000	0.0070 (8)	0.000
C8	0.0296 (9)	0.0474 (11)	0.0324 (10)	0.000	0.0009 (7)	0.000
C9	0.0318 (9)	0.0313 (9)	0.0316 (10)	0.000	0.0052 (7)	0.000
C10	0.0309 (9)	0.0319 (9)	0.0315 (9)	0.000	0.0049 (7)	0.000
C11	0.0427 (11)	0.0474 (12)	0.0386 (11)	0.000	0.0135 (9)	0.000
C12	0.0453 (12)	0.100 (2)	0.0449 (12)	0.000	0.0190 (10)	0.000

C13	0.0358 (10)	0.0567 (13)	0.0410 (11)	0.000	0.0124 (9)	0.000
C14	0.0490 (12)	0.0812 (17)	0.0417 (12)	0.000	0.0182 (10)	0.000
N1	0.0329 (8)	0.0573 (11)	0.0288 (8)	0.000	0.0068 (7)	0.000
N2	0.0319 (8)	0.0539 (10)	0.0301 (8)	0.000	0.0062 (6)	0.000
O1	0.0463 (9)	0.1019 (14)	0.0327 (8)	0.000	0.0100 (7)	0.000
O2	0.0324 (8)	0.201 (3)	0.0432 (9)	0.000	0.0078 (7)	0.000
O3	0.0803 (9)	0.0778 (9)	0.0545 (7)	0.0232 (7)	−0.0123 (6)	0.0131 (6)

Geometric parameters (Å, °)

C1—C2	1.370 (3)	C8—C9	1.410 (3)
C1—C9	1.405 (3)	C8—H8	0.9300
C1—H1	0.9300	C9—C10	1.418 (2)
C2—C3	1.413 (3)	C11—O1	1.212 (2)
C2—C11	1.496 (3)	C11—C12	1.490 (3)
C3—C4	1.359 (3)	C12—H12A	0.9328
C3—H3	0.9300	C12—H12B	0.9534
C4—C10	1.414 (3)	C13—O2	1.192 (3)
C4—H4	0.9300	C13—N2	1.367 (2)
C5—C6	1.374 (3)	C13—C14	1.484 (3)
C5—C10	1.410 (3)	C14—H14A	0.8470
C5—N1	1.468 (2)	C14—H14B	0.9329
C6—N2	1.402 (2)	N1—O3	1.2038 (14)
C6—C7	1.421 (3)	N1—O3 ⁱ	1.2038 (14)
C7—C8	1.356 (3)	N2—H2	0.8600
C7—H7	0.9300		
C2—C1—C9	121.65 (17)	C1—C9—C8	122.63 (17)
C2—C1—H1	119.2	C1—C9—C10	119.02 (17)
C9—C1—H1	119.2	C8—C9—C10	118.35 (17)
C1—C2—C3	118.58 (17)	C5—C10—C4	123.87 (17)
C1—C2—C11	119.07 (18)	C5—C10—C9	117.26 (16)
C3—C2—C11	122.34 (17)	C4—C10—C9	118.87 (17)
C4—C3—C2	121.69 (18)	O1—C11—C12	120.52 (18)
C4—C3—H3	119.2	O1—C11—C2	120.13 (18)
C2—C3—H3	119.2	C12—C11—C2	119.35 (18)
C3—C4—C10	120.19 (17)	C11—C12—H12A	111.2
C3—C4—H4	119.9	C11—C12—H12B	108.9
C10—C4—H4	119.9	H12A—C12—H12B	108.6
C6—C5—C10	124.35 (16)	O2—C13—N2	122.84 (19)
C6—C5—N1	119.30 (16)	O2—C13—C14	121.53 (19)
C10—C5—N1	116.35 (15)	N2—C13—C14	115.63 (17)
C5—C6—N2	120.69 (16)	C13—C14—H14A	113.9
C5—C6—C7	116.93 (16)	C13—C14—H14B	111.7
N2—C6—C7	122.38 (16)	H14A—C14—H14B	107.9
C8—C7—C6	120.58 (17)	O3—N1—O3 ⁱ	123.93 (18)
C8—C7—H7	119.7	O3—N1—C5	118.03 (9)
C6—C7—H7	119.7	O3 ⁱ —N1—C5	118.03 (9)

C7—C8—C9	122.54 (17)	C13—N2—C6	127.79 (16)
C7—C8—H8	118.7	C13—N2—H2	116.1
C9—C8—H8	118.7	C6—N2—H2	116.1
C9—C1—C2—C3	0.000 (1)	N1—C5—C10—C9	180.000 (1)
C9—C1—C2—C11	180.000 (1)	C3—C4—C10—C5	180.000 (1)
C1—C2—C3—C4	0.000 (1)	C3—C4—C10—C9	0.0
C11—C2—C3—C4	180.000 (1)	C1—C9—C10—C5	180.000 (1)
C2—C3—C4—C10	0.000 (1)	C8—C9—C10—C5	0.0
C10—C5—C6—N2	180.000 (1)	C1—C9—C10—C4	0.000 (1)
N1—C5—C6—N2	0.000 (1)	C8—C9—C10—C4	180.0
C10—C5—C6—C7	0.000 (1)	C1—C2—C11—O1	0.000 (1)
N1—C5—C6—C7	180.000 (1)	C3—C2—C11—O1	180.000 (1)
C5—C6—C7—C8	0.000 (1)	C1—C2—C11—C12	180.000 (1)
N2—C6—C7—C8	180.000 (1)	C3—C2—C11—C12	0.000 (1)
C6—C7—C8—C9	0.000 (1)	C6—C5—N1—O3	90.34 (15)
C2—C1—C9—C8	180.000 (1)	C10—C5—N1—O3	−89.66 (15)
C2—C1—C9—C10	0.000 (1)	C6—C5—N1—O3 ⁱ	−90.34 (15)
C7—C8—C9—C1	180.000 (1)	C10—C5—N1—O3 ⁱ	89.66 (15)
C7—C8—C9—C10	0.000 (1)	O2—C13—N2—C6	0.000 (1)
C6—C5—C10—C4	180.000 (1)	C14—C13—N2—C6	180.000 (1)
N1—C5—C10—C4	0.000 (1)	C5—C6—N2—C13	180.000 (1)
C6—C5—C10—C9	0.000 (1)	C7—C6—N2—C13	0.000 (1)

Symmetry code: (i) $x, -y+3/2, z$.

Hydrogen-bond geometry (\AA , $^\circ$)

$D-H\cdots A$	$D-H$	$H\cdots A$	$D\cdots A$	$D-H\cdots A$
N2—H2 \cdots O1 ⁱⁱ	0.86	2.35	3.177 (2)	161
C7—H7 \cdots O2	0.93	2.18	2.792 (2)	123
C4—H4 \cdots O2 ⁱⁱⁱ	0.93	2.34	3.219 (2)	157

Symmetry codes: (ii) $x, y, z+1$; (iii) $x+1, y, z$.